Diffractive $D^{*\pm}(2010)$ Production in Deep Inelastic Scattering from ZEUS

J. E. Cole[a] (On behalf of the ZEUS Collaboration)

[a]HEP Group, Imperial College of Science, Technology and Medicine, Blackett Laboratory, Prince Consort Road, London, SW7 2BZ, UK.

Measurements of diffractive $D^{*\pm}$ production in deep inelastic scattering using the 1995 – 1997 ZEUS data are presented. Diffractive $e^+p \to e^+XN$ interactions are identified by the presence of a large rapidity gap in the final state. $D^{*\pm}$ candidates are identified from the $D^* \to D^0\pi$ decay mode, where the D^0 subsequently decays either to $K^-\pi^+$ + (c.c.) or $K^-\pi^+\pi^-\pi^+$ + (c.c.). The integrated $D^{*\pm}$ cross section along with differential $D^{*\pm}$ cross sections as a function of Q^2, W, $x_{I\!P}$, $p_T(D^{*\pm})$ and $\eta(D^{*\pm})$ have been measured in a limited kinematic region. The fraction of $D^{*\pm}$ events produced diffractively has also been measured.

1. INTRODUCTION

Open charm production is a key process through which the nature of diffractive interactions at HERA may be probed. This is principally due to the large charm mass which, by providing a hard scale, allows the comparison of the measurement with perturbative Quantum Chromodynamics (pQCD). Open charm production is also free from the theoretical uncertainties associated with the production of bound states, such as the J/ψ meson.

Another crucial aspect of charm production is its sensitivity to the presence of gluons in the interaction, as observed in non-diffractive deep inelastic scattering (DIS) [1,2]. This is particularly important in diffraction as it helps to discriminate between different models. These include the so-called "Resolved Pomeron ($I\!P$)" model [3], the pQCD models [4–6] and the soft colour interaction (SCI) models [7,8]. The latter two predict that charm production will be suppressed at leading order, but it has been suggested that this is compensated for by the inclusion of real and virtual gluon corrections [5,6,8]. The first model predicts unsuppressed charm production if the pomeron consists predominantly of gluons, but predicts the suppression of charm production if the pomeron consists of quarks.

2. EVENT SELECTION

Selection methods [2] are used to identify DIS events which contain a $D^{*\pm}$ candidate which decayed through either of the following channels

$$D^{*+} \to D^0\pi^+ \to (K^-\pi^+)\pi^+ + \text{(c.c.)} \quad (1)$$

$$D^{*+} \to D^0\pi^+ \to (K^-\pi^+\pi^-\pi^+)\pi^+ + \text{(c.c.)}\ . \quad (2)$$

From these events, those with a large rapidity gap in the outgoing proton direction are selected by requiring that the pseudorapidity of the forwardmost energy cluster (which must have an energy of at least 0.4 GeV), η_{max}, should be less than some value η_{cut}. For the 3-prong decay channel (1), $\eta_{cut} = 1.5$, while for the 5-prong decay channel (2), $\eta_{cut} = 2.0$. This method of selecting diffractive photon dissociative events selects a sample containing little non-diffractive background, but suffers from a significant background contribution from proton dissociative events. This has been estimated from inclusive diffractive ZEUS results to be 31 ± 15 % [9].

3. INCLUSIVE $D^{*\pm}$ CROSS SECTIONS

3.1. The 5-prong decay channel

The measurements from decay channel (2) have been made using the 1996-1997 ZEUS dataset ($\mathcal{L}$ = 37 pb^{-1}). Candidates have been selected from the kinematic region defined by $1 < Q^2 < 480$ GeV^2 (Q^2 is the square of the four-momentum transfer at the leptonic vertex), $0.04 < y < 0.7$ (y is the fractional energy transfer from the positron to the hadronic system in the proton rest frame), $2 < p_T(D^{*\pm}) < 9$ GeV ($p_T(D^{*\pm})$ is the transverse momentum of the $D^{*\pm}$), $|\eta(D^{*\pm})| < 1.5$, $x_{\mathbb{P}} < 0.015$ ($x_{\mathbb{P}} = \frac{Q^2+M_X^2}{Q^2+W^2}$ is the fraction of the proton momentum carried by the pomeron, with M_X defined as the invariant mass of the final state X into which the photon dissociates) and $\beta < 0.8$ ($\beta = \frac{Q^2}{Q^2+M_X^2}$). All pseudorapidities and transverse momenta have been measured in the lab frame. The resulting $D^{*\pm}$ signal was found to contain 121 ± 24 signal candidates. These data were then corrected for detector acceptance using Monte Carlo events generated with RAPGAP [10] (based on the resolved pomeron model) which gives a reasonable description of the data from both decay channels. The cross section for diffractive $D^{*\pm}$ production in the kinematic region defined above was then measured to be

$$\sigma(e^+p \to e^+D^{*\pm}Xp) = 526 \pm 110^{+200}_{-240} \text{ pb.} \qquad (3)$$

3.2. The 3-prong decay channel

The results for decay channel (1) are extracted from the full 1995-1997 dataset ($\mathcal{L} = 43.3$ pb^{-1}). The candidates for this decay channel have been selected from a significantly different kinematic region, compared with that defined in section 3.1, which is defined by $3 < Q^2 < 150$ GeV^2, $0.02 < y < 0.7$, $p_T(D^{*\pm}) > 1.5$ GeV, $|\eta(D^{*\pm})| < 1.5$, $0.002 < x_{\mathbb{P}} < 0.012$ and $\beta < 0.8$. Here the $D^{*\pm}$ signal was found to contain 59 ± 9 candidates. These data were then corrected for acceptance yielding a cross section for this kinematic region of

$$\sigma(e^+p \to e^+D^{*\pm}Xp) = 379 \pm 66^{+99}_{-140} \text{ pb.} \qquad (4)$$

In order to compare this result to (2) measured from the 5-prong decay channel, result (2) was interpolated to the kinematic region described in section 3.1 using Monte Carlo simulations. This resulted in a diffractive $D^{*\pm}$ cross section of

$$\sigma(e^+p \to e^+D^{*\pm}Xp) = 398 \pm 83^{+154}_{-180} \text{ pb.} \qquad (5)$$

which is in excellent agreement with the result from the 3-prong decay channel.

4. DIFFERENTIAL CROSS SECTIONS AND RATIOS

Differential $D^{*\pm}$ cross sections were measured from decay channels (1) and (2) as a function of Q^2, W, $x_{\mathbb{P}}$, $p_T(D^{*\pm})$ and $\eta(D^{*\pm})$ and are shown in figures 1 and 2. In each plot the results are compared to three different theoretical predictions. The solid line indicates the predictions of the Buchmüller, Hebecker and McDermott (BHM) soft colour interaction model [8], while the dashed line indicates the predictions made by Alvero et al. (ACTW), which are based on a gluon-dominated resolved pomeron model which has been fitted to a range of ZEUS and H1 results [11]. Finally, the dotted line shows the predictions of the Ryskin pQCD model as implemented in the RIDI Monte Carlo generator [6,12]. This includes higher order corrections, which are known to cause a large normalisation uncertainty in the predictions. For this reason, the predictions from RIDI have been normalised to the data cross section. All three models appear to de-

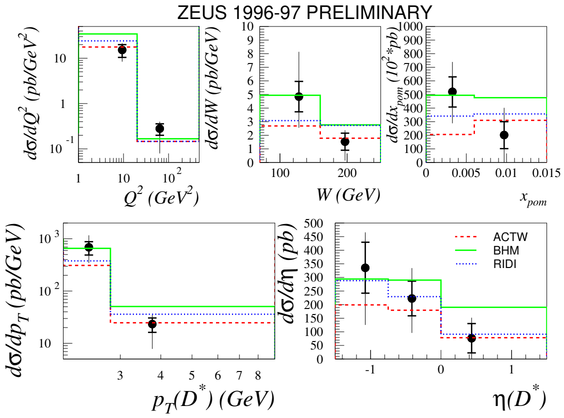

Figure 1. The differential cross sections measured from the 5-prong decay channel versus Q^2, W, $x_{\mathbb{P}}$, $p_T(D^{*\pm})$ and $\eta(D^{*\pm})$. The dots are the data points, whose inner error bars indicate the statistical errors only. The outer error bars are the statistical and systematic errors added in quadrature.

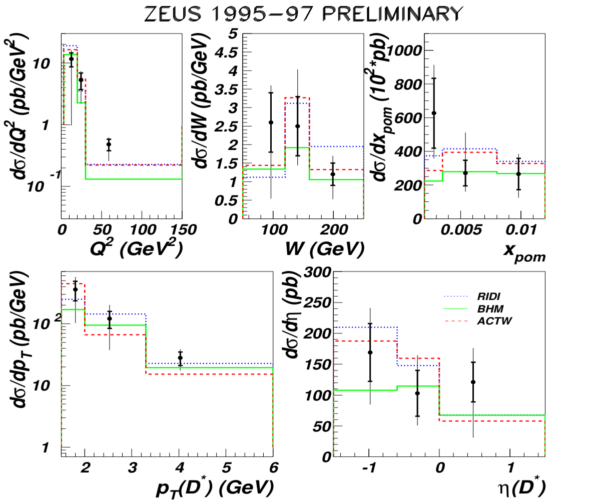

Figure 2. The differential cross sections measured from the 3-prong decay channel versus Q^2, W, $x_{\mathbb{P}}$, $p_T(D^{*\pm})$ and $\eta(D^{*\pm})$. The dots are the data points, whose inner error bars indicate the statistical errors only. The outer error bars are the statistical and systematic errors added in quadrature.

scribe the data reasonably well, but more statistics are clearly required in order to discriminate between the different models.

The ratio (R) of diffractive $D^{*\pm}$ to total $D^{*\pm}$ production has also been measured from the 5-prong decay channel to be

$$R = 8.9 \pm 2.4^{+1.7}_{-1.6}\% \tag{6}$$

and from the 3-prong decay channel to be

$$R = 7.0 \pm 1.3^{+1.7}_{-1.8}\%. \tag{7}$$

These values are in good agreement, even though the results are measured in substantially different kinematic regions. They are also consistent with the fraction of the total cross section attributed to diffractive scattering [9], indicating that diffractive charm production is not suppressed.

The dependence of this ratio on W and Q^2 has been measured from the 3-prong decay channel. It is illustrated in figure 3 and is flat within errors.

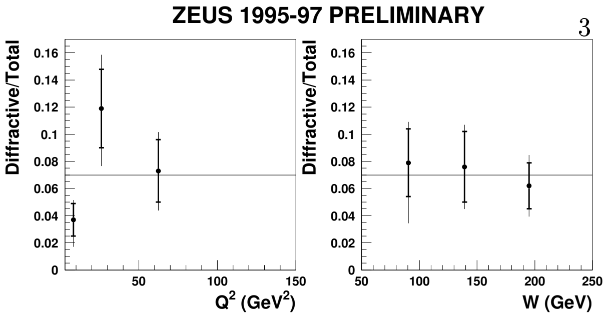

Figure 3. The ratio of diffractive $D^{*\pm}$ to total $D^{*\pm}$ as a function of Q^2 and W measured from the 3-prong decay channel. The inner error bars indicate the statistical error on the data points, while the outer error bars indicate the statistical and systematic errors added in quadrature. The line indicates the ratio quoted in equation (6).

REFERENCES

1. C. Adloff et al., Z. Phys. **C72** (1996) 593.
2. J. Breitweg et al., Phys. Lett. **B407** (1997) 402; I. Redondo, these proceedings.
3. G. Ingelman and P. Schlein, Phys. Lett **B152** (1985) 256; A. Donnachie and P. Landshoff, Phys. Lett. **B191** (1987) 309, Phys. Lett. **B198** (1987) 590(E).
4. N. N. Nikolaev and B. G. Zakharov, Z Phys. **C53** (1992) 331; M. Genovese, N. N. Nikolaev and B. G. Zakharov, Phys. Lett. **B378** (1996) 347; J. Bartels and M. Wüsthoff, J. Phys G: Nucl. Part. Phys. **22** (1996) 929.
5. E. M. Levin et al., hep-ph/9606443 (1996).
6. M. G. Ryskin, Sov. J. Nucl. Phys. **52** (1990) 529.
7. A. Edin, G. Ingelman and J. Rathsman, Phys. Lett. **B366** (1996) 371; W. Buchmüller and A. Hebecker, Phys. Lett. **B355** (1995) 573.
8. W. Buchmüller, A. Hebecker and M. F. McDermott, hep-ph/9607290.
9. J. Breitweg et al., Euro. Phys. J **C6** (1999) 43.
10. H. Jung, Comp. Phys. Comm. **86** (1995) 147.
11. L. Alvero et al., hep-ph/9805268 (1998); hep-ph/9806340 (1998).
12. M. G. Ryskin, S. Y. Sivoklokov and A. Solano, Proc. of the Int. Conf. on Elastic and Diffractive Scattering, Ed. H. M. Fried et al., (1993), World Scientific; A. Solano, Proc. of the Monte Carlo Workshop, Ed. G. Grindhammer et al., (1998-99) DESY.